International Journal of Research in Advanced Engineering and Technology
ISSN: 2455-0876; Impact Factor: RJIF 5.44
www.newengineeringjournal.in
Volume 3; Issue 2; May 2017; Page No. 79-83

Sensor results from pendulum swing and outlooks for cricket bat swing parameterizations

Ajay K Sarkar

Department of EEE, RUET, Rajshahi-6204, Bangladesh

Abstract
The use of sensors is now achieving rigorous attention in cricket research. Attaching a triaxial accelerometer sensor to a rigid wooden pendulum, the tilted and deflection angles during its stationary and swing position was investigated. The tilted angles at different static steps and swing angles were measured using the sensor output and compared with inclinometer readings (static case) and with those estimated using the solution of a damped pendulum equation (swing case) and a good agreement were obtained (r = 0.99, p<0.0001 and r = 0.88, p<0.0001 respectively). The wooden pendulum was not frictionless, a correction was attempted by choosing varying damping constant for the equation and improved matching obtained (r = 0.91) with the improved slope of the regression line. The bias error was also attempted to minimize. This study foresights that the damping constant could be a criterion to measure swing inertia related parameters in cricket batting research.

Keywords: sensor, pendulum, damping constant, acceleration spikes

1. Introduction
The application of accelerometer sensors is emerging as a popular method of biomechanical quantification of health and sportive activity [1]. Fallon *et al* [2]. assessed the applicability of five different types of sensor to identify impact location of baseball and bat and the swing speed of the bat. They found accelerometer and microphone sensors were the most promising, however, relative levels of the signals were used for comparison among the sensors. This study did not consider sensor errors but compared the sensor results. This means that although accelerometers have some errors in some motion measurements, the value of errors in many cases can be neglected if a gross relationship with movement parameters is sought or comparison is made among movements and sensor recorded signals. Several works have reported methods to minimize sensor error. Sipos *et al* [3]. Proposed a calibration procedure for a triaxial accelerometer relying on optimal position and sensor number for minimizing cost and process time. They also compared three calibration algorithms applicable to triaxial accelerometers to determine a mathematical error model. In 2008, Tan *et al* [4]. proposed a solution for the estimation of drift free displacement of periodic motion from inertial sensors. This method is limited to periodic motion. Suh [5] in 2012 proposed a new smoother method to estimate attitude and position of movement to be less sensitive to the uncalibrated sensor parameters and sensor noise. In that work using two boundary information (zero velocity interval), the attitude was estimated using a smoother as a combination of forward and backward filter. The velocity was estimated by a velocity smoother using the smoothed attitude. That study computed the position by integrating the estimated velocity. The proposed method is suitable for analysis of movement for short time intervals only.
In this study, triaxial accelerometer sensor revealed signals were used to measure the angles at different static tilted position and the swing position of a wooden pendulum. The results were checked by inclinometer and equation by calculating the correlation between the sensor's results and those from equation and inclinometer and the correction was attempted.

2. Experimental procedure
An inertial sensor is a module or platform used as a motion sensing device. Accelerometers and gyroscopes are two types of such devices of which the first one is used for linear and the second is used for angular acceleration measurements along three axes of the three dimensional spaces. The motion related data are converted to electrical signals. One of the basic mechanisms of measuring the acceleration is by converting the motion to a change in the electrical parameters within these sensors. The small sensors commonly use some form of Micro-Electro-Mechanical Systems (MEMS). These systems work by detecting the change in position of a suspended mass relative to the body as a change in capacitance. The sensors are commonly manufactured in silicon, and its body, proof-mass, the suspended systems are silicon, with the components etched in the silicon using similar techniques to semiconductor manufacture. Each sensor platform is composed of a readily available low cost microprocessor and features on-board memory, inertial sensors, and USB (Universal Serial Bus) communications. The accelerometer sensor platform contains two embedded inertial sensors; each is capable of measuring accelerations in two perpendicular directions. This facilitates collection of data in three dimensional spaces. One of a typical accelerometer sensor platforms (devised by Davey *et al*. [6] in 2008, the architecture and operating system were also outlined) capable of measuring 6g was attached by tape to the swing arm of the wooden pendulum as shown in Fig. 1.

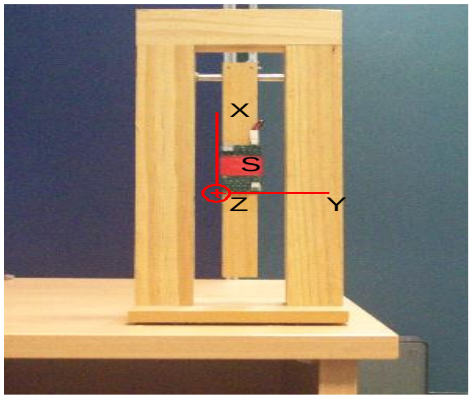

Fig 1: Sensor (S) attached wooden pendulum and definition of sensor's axes. The centre wooden part is free to rotate about a horizontal axis (metal rod).

The sensors axes (X, Y, and Z) are shown in the Fig. 1 and the swing of the pendulum was along the Z-axis direction in the ZX plane (perpendicular to the ground YZ-plane). The pendulum was oriented at a fixed angle to the vertical and released. The subsequent oscillations were recorded using the accelerometer. The swing arm was initially stationary at different angle steps (-3º, 0º, 6º, 9º, 25º, 45º, 75º, 90º) measured by an inclinometer (vertical axis reference). The arm was oriented so that the sensor Z-axis was in the same direction as gravity (opposite to positive swing direction) before allowing the pendulum to swing freely. The negative angle for first step was due to the fact that the swing arm was not precisely vertical at rest. At the last step (90º) with sensor Z-axis aligned with gravity, the swing arm was released for free swing. The X-, Y- and Z-axis acceleration data were recorded during the different angular static positions and free swing position of the pendulum arm.

3. Result and Discussion

Fig. 2 shows the X-, Y- and Z-axis acceleration profiles (A_x, A_y, and A_z) from the static experiment. The magnitude of the average acceleration of each of A_x and A_z during each step was used to calculate the tilted angles θ_X and θ_Z using cosine and sine function respectively. The angles shown in Fig. 2 were measured by the inclinometer.

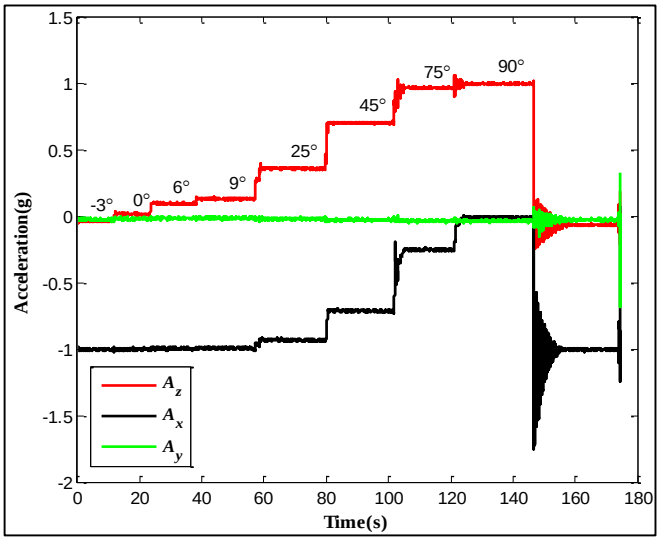

Fig 2: Sensor recorded acceleration in tilted and swing position of the wooden pivot arm. The tilted angles in each step were measured by inclinometer.

Table 1 shows the value of the angles measured by inclinometer (θ_I) and accelerometer (θ_X, θ_Z using X-axis and Z-axis acceleration respectively) using the data shown in Fig. 2 in the tilted position of the pivot arm. To assess the strength of the relationship between inclinometer measured angles and those measured by accelerometer, θ_X, and θ_Z were plotted against θ_I shown in Fig. 3. A strong linear relationship between θ_I and θ_X (r_x = 0.9932, p<0.0001) and between θ_I and θ_Z (r_z = 0.9969, p<0.0001) was obtained. However, the relationship was checked within 0º to 90º, but it is noted that at the start (around 0º)

Table 1: Accelerometer and inclinometer measured angles during tilted positions of the pivot arm

	Step-1	Step-2	Step-3	Step-4	Step-5	Step-6	Step-7	Step-8
θ_I (degree)	-3	0	6	9	25	45	75	90
θ_X (degree)	0	0	3.35	6.31	20.94	44.38	75.29	89.19
θ_Z (degree)	2.32	0.86	5.32	7.37	20.86	44.32	74.27	83.52

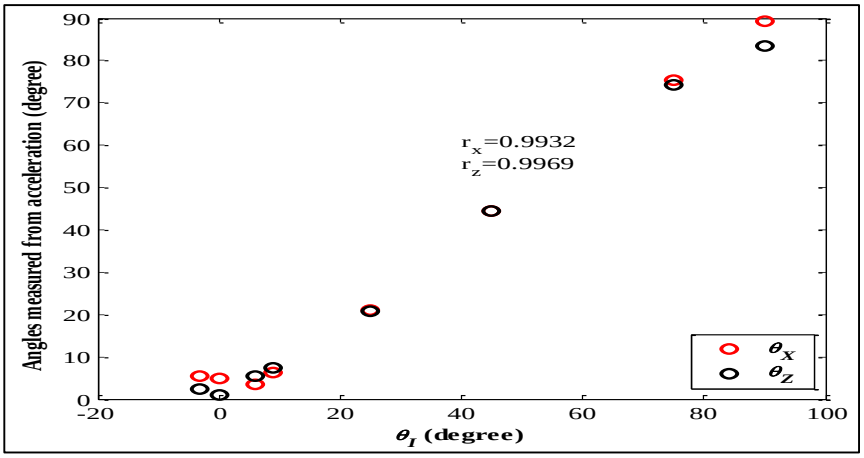

Fig 3: Inclinometer measured angles (θ_I) versus those measured from acceleration data (θ_X from X-axis acceleration, θ_Z from Z-axis acceleration) for stationary tilted arm. The correlation coefficients shown in the figure as r_x and r_z are between θ_I and θ_X and between θ_I and θ_Z respectively.

and end (around 90º) of the plot in Fig. 3 the data diverts slightly from the linear relationship. This tendency indicates that if the measured range could be extended the profile would exhibit some degree of the nonlinearity resulting from the sensor sensitivity error [7] as evident in Fig. 4.

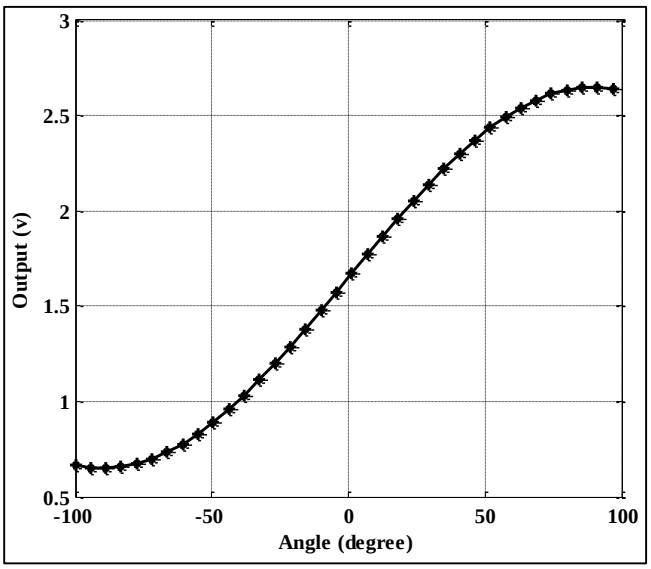

Fig 4: Typical nonlinear output in voltage of the X-axis of a typical accelerometer with respect to its alignment to gravity (Freescale semiconduct inc., 2005 [7]).

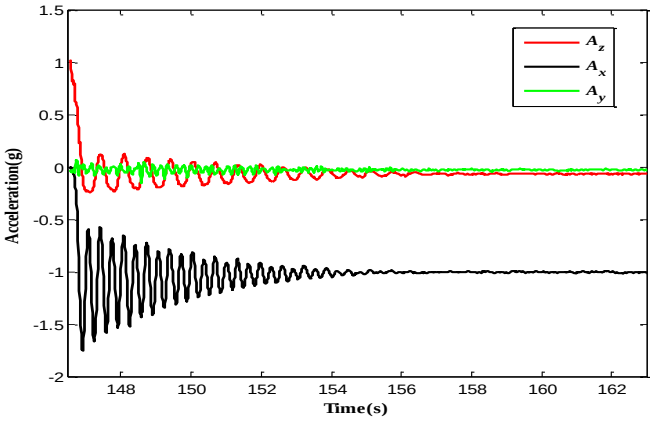

Fig 5: (a) Expanded version of the acceleration of the wooden pivot arm during the swing shown in Fig. 2.

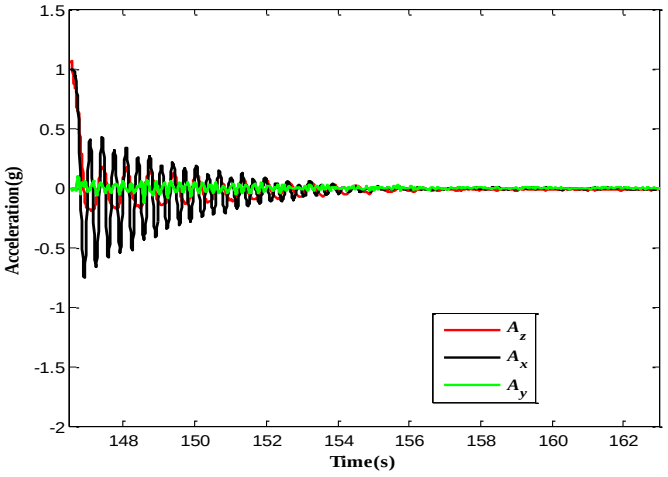

Fig 5: (b) DC bias removed version of the acceleration shown in Fig. 5(a).

The acceleration during the swing position is shown in Fig. 5(a) as an expanded version of Fig. 2. The swing starts at 90º (the pendulum arm is parallel to ground and normal to gravity) with Z-axis aligned and X-axis normal to the gravity direction. A_z and A_x have the values 1g and 0g value as seen in Fig. 5(a). The A_z profile indicates that the pendulum does not swing symmetrically about the 0g axis and does not converge to 0g acceleration at the end of the swing. This is due to the -3º offset at rest. As a first approximation the

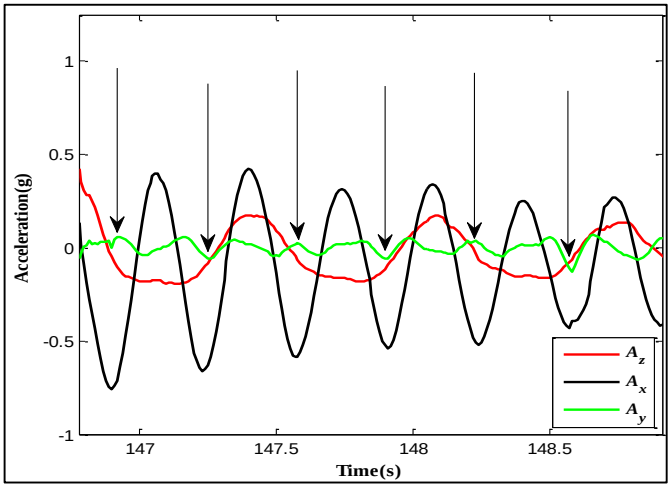

Fig 5: (c) Expanded version of the acceleration during several cycles as shown in Fig. 5(b).

data was corrected by subtracting from A_z. However, any bias observed in A_y is due to either imperfections of the pendulum structure (e.g. friction which is angle dependent) that leads to Y-axis having movement or cross-axis error within the sensor. Fig. 5(b) shows all the three profiles of Fig. 5(a) with the bias offset removed and from A_y by subtracting its mean value. The mean value of A_y shown in Fig. 5(a) is -0.0276g and when converted to angle using cosine function it gives 91.58º. So the sensor's Y-axis is not exactly 90º with the swing plane. As seen from Fig. 5(b) all the accelerations converge to 0g acceleration at the end of the swing. A close inspection of the first several cycles from Fig. 5(b) reveals that A_y has values (Fig. 5(c)) that arise from the wooden structure manufacturing error or cross-axis error.

As seen in Fig. 5(c), at each peak value of A_y (indicated by arrow), A_x has a larger peak compared to the other peaks (positive) while A_y has steady changes around zero. A_x is not symmetric between the positive and negative peaks. Another observation in Fig. 5(c) indicates that the swing frequency of A_x and A_z are different. This difference is obvious as the centripetal acceleration, A_x is proportional to the square of angular velocity, so its frequency differs from the value of the swing angle frequency, but the frequency of tangential acceleration, A_z does not differ. Because A_z is proportional to the angular acceleration, that is the second order derivative of the swing angle, and then the frequency of A_z remains the same as in swing angle.

The general equation of the swing angles (θ) as a solution of a damped pendulum equation is given as follows [8]:

$$\theta = Be^{-kt}\cos(ht) + Ae^{-kt}\sin(ht) \quad (1)$$

where A and B are the constants and k, h, t are the damping constant, angular swing frequency and time respectively.

Differentiating Eq. 1 gives an expression for the angular velocity:

$$\frac{d\theta}{dt} = (Bh - Ak)e^{-kt}\cos(ht) - (Ah + Bk)e^{-kt}\sin(ht) \quad (2)$$

To calculate the swing angle from the profile shown Fig. 5(a), an FT (Fourier Transform) of the acceleration profile was used to estimate the dominant frequency. This allows the gravity components to be removed. Fig. 6 shows the FT of a 1024 sample window calculated using the FFT (Fast Fourier Transform) in the ADAT tool box [9]. It is observed from Fig. 6 that 1.5 Hz, 2.3 Hz, 0.73 Hz frequency

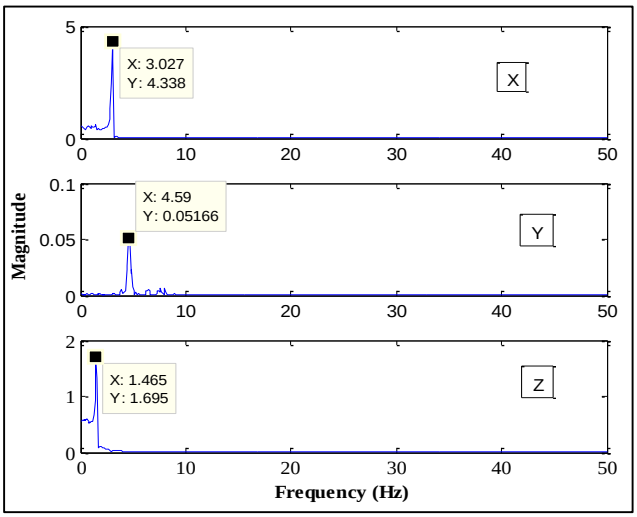

Fig 6: FT of the acceleration profile shown in Fig. 5(a). FFT was calculated using ADAT tool box developed by [9] taking 1024 data points window.

are low enough for the low pass filters to extract the gravity components in X-, Y- and Z-axis respectively according to [10], assuming that artifact related low frequency signal is approximately zero. A Butterworth filter was used to extract the gravity components. The order of the filter and the Butterworth natural frequency for each axis was determined using the 'buttord' function in MATLAB software allowing less than 3 db losses in the pass-band and at least 60 db attenuations in the stop-band. Fig. 7 shows the angles during the swing (θ) calculated using the gravity acceleration components (A_{gx}, A_{gy} and A_{gz}) by pitch angles using the calculation method described by Bai *et al.*, 2012 [11]:

$$\theta = \arctan\left(\frac{A_{gz}}{\sqrt{A_{gx}^2 + A_{gy}^2}}\right) \quad (3)$$

The upper part of Fig. 7 shows the calculated angles from the low-pass filtered data using Eq. 3 and the lower part the calculated angles with off-set removed. As mentioned above the off-set resulted from the fact the pivot arm was not perfectly vertically aligned at rest due to the weight of the dc battery pack attached to the arm for sensor.

To compare the sensor estimated angles with those from Eq. 1, the constants *A*, *B*, *h* and *k* were calculated in the followings ways:

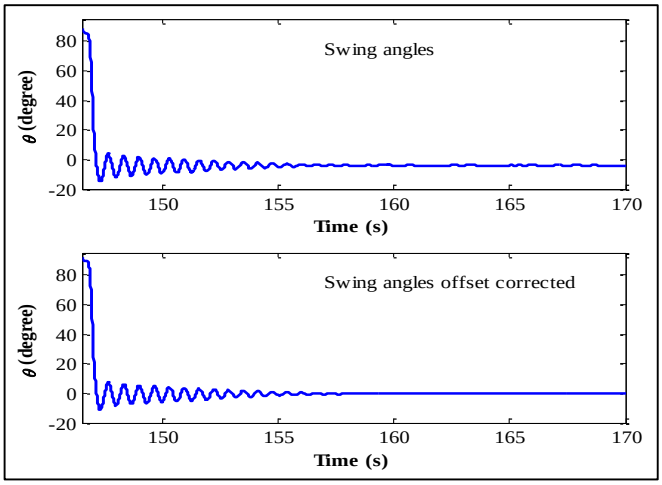

Fig 7: Swing angles of the pendulum calculated from the gravity acceleration component in each axis by the pitch angle calculation method as stated by Bai *et al.*, 2012 [11].

At $t = 0$ (start of the swing), θ is the initial angles of the swing. In this case the first positive angle peak (7.87º) in the swing profile in the upper part of Fig. 7 was chosen instead of the beginning angle (90º). This choice was made because at the beginning the pendulum arm was released by human hand and the release is not well controlled. So at this first positive peak, the angle and angular acceleration are 7.87º and 0 respectively. Putting $t = 0$ and these two values in Eq. 1 and 2 we obtain:

$$B = 7.87\,,\ Ak = Bh \quad (4)$$

The angular swing frequency *h* can be estimated from the FFT of the swing angle profile

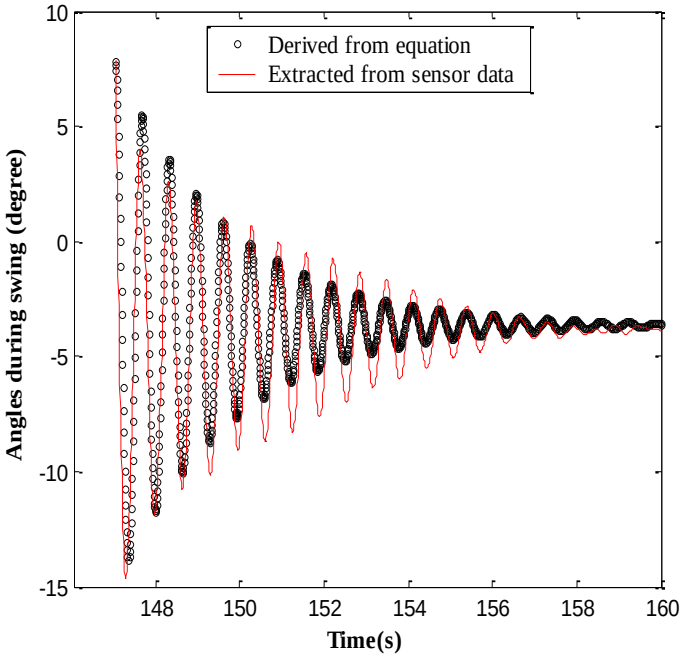

Fig 8: Swing angles of the calculated from sensor data and estimated from equation.

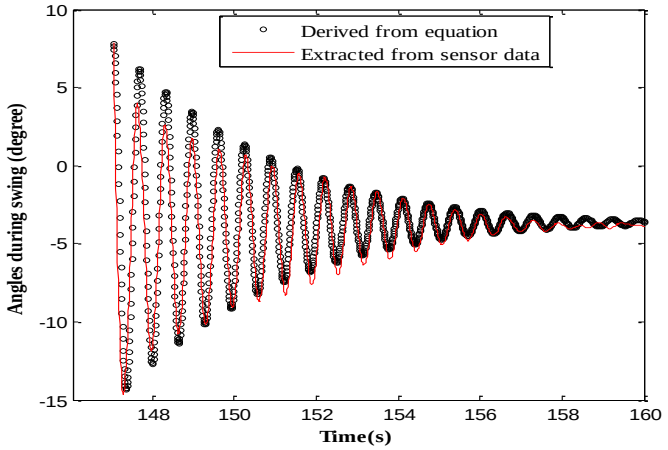

Fig 9: Swing angles of the calculated from sensor data and estimated from equation with a variable damping constant shown in Fig. 10.

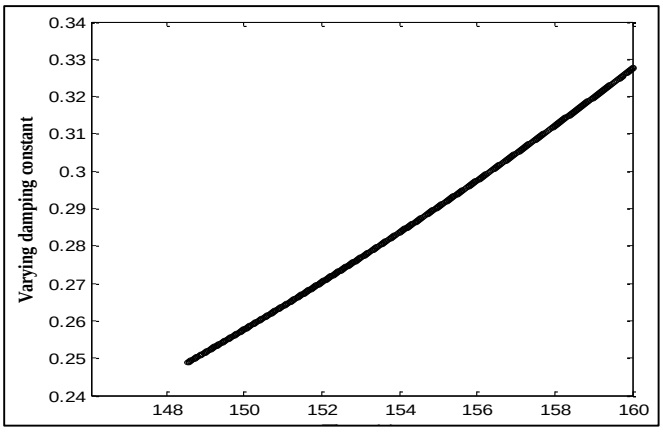

Fig 10: A variable damping constant used in the equation for after 150 points to derive swing angle profile as shown in Fig. 8.Variable constant were taken to minimize the magnitude difference between equation and sensor profiles observed in Fig. 8, however, a constant damping constant was used for first 150 points.

in Fig. 7 starting from the first positive peak. The FFT analysis (using a 1024 data window) gives the frequency 1.56 Hz, and then the value of h is 9.8. The damping constant k was estimated from the values of positive peaks of A_z profile in Fig. 5(a) using an logarithmic fit. As the profile follows a regular shape, the peak values were extracted using an algorithm written in Matlab R2008a (www.mathwork.com). Substituting the values of h, B, and k in Eq. 4 the value of A was determined. The equation derived and sensor revealed swing angle profiles are shown in Fig. 8. The angles showed good agreement (correlation coefficient, r = 0.88). However the amplitude differed after first several cycles in both upward and downward peaks from 150.01s to 155.12s. Taking a variable damping constant of which the first 150 points is constant (from the logarithmic fit) and the rest as a increasing exponential function of time, the differences between the profiles (150.01s~155.12s) were minimized (see Fig. 9).

The exponential damping constant was chosen using trial and error around the value from logarithmic fit (Fig. 10). In this case the correlation coefficient between the equation and sensor angles improved (r = 0.91) compared to the former case (r = 0.88). Also the slope of the regression line improved to 0.97 compared to the previous slope of 0.83.

4. Conclusions

The pendulum swing was used to investigate the angles from the static and swing positions of the sensor. Static angles from sensor data were compared with inclinometer angles and found good agreement (r = 0.99). The swing angles (calculated from sensor data) were compared with angles estimated by the solution of a damped pendulum equation imposing the conditions for the constants. A good agreement between the two angle profiles (from sensor data and from the equation) were obtained (r = 0.88). An attempt was made to improve the matching of those two profiles by taking a varying damping constant and obtained an enhanced correlation coefficient, r = 0.91 and the slope of the regression line 0.97 instead of 0.83 in the former case. The damping constant can be a criterion to measure of the applied force by the batter in the straight drive bat swing in cricket. How much swing inertia is overcome by the batters can be quantified by measuring this constant in matching the sensor and equation derived data.

5. Acknowledgments

This work was conducted as part of the author's Ph. D. program and is supported with GUPRS and GUIPRS scholarships granted by Griffith University, Australia.

6. References

1. James DA, Davey N, Rice T. An accelerometer based sensor platform for insitu elite athlete performance analysis, IEEE Sensor. Vienna, Austria. 2004, 1373-1376.
2. Fallon L, Sherwood J, Donaruma M. An Assessment of Sensing Technologies to Monitor the Collision of a Baseball and Bat (P34), the Engineering of Sport. Springer Paris. 2008, 191-198.
3. Sipos M, Paces P, Rohac J, and Novacek P. Analyses of triaxial accelerometer calibration algorithms, IEEE SENSORS JOURNAL. 2012; 12:1157-1165.
4. Tan UX, Veluvolu KC, Latt WT, Shee CY, Riviere CN, and Ang WT. Estimating displacement of periodic motion with inertial sensors, Ieee Sensors Journal. 2008; 8:1385-1388.
5. Suh YS. A Smoother for Attitude and Position Estimation Using Inertial Sensors with Zero Velocity Intervals, IEEE SENSORS JOURNAL. 2012; 12:1255-1262.
6. Davey N, Wixted A, Ohgi Y, James DA. A low cost self-contained platform for human motion analysis, The Impact of Technology on Sport II. 2008, 101-111.
7. http://www.freescale.com, 2012.
8. www.math.vt.edu/people/renardy/class_home/FromSun/ade_ch2.pdf, 2012.
9. James DA and Wixted A. ADAT: A Matlab toolbox for handling time series athlete performance data, Procedia Engineering. 2011; 13:451-456.
10. Wixted AJ. In-situ Athlete Monitoring: Data Collection, Interpretation & Feature Extraction, Doctor of Philosophy. Griffith School of Engineering, Griffith University, Brisbane, Australia, 2007.
11. Lu B, Pepper MG, Yana Y, Spurgeon SK, Sakel M. Application of low cost inertial sensors to human motion analysis, in the Proceedings of 2012 IEEE International Instrumentation and Measurement Technology Conference (I2MTC). 2012; 1280-1285.